

CrossMark  
click for updates

Cite this: DOI: 10.1039/c5nj01821h

# An anti-biodegradable hydrophobic sulfonate-based acrylamide copolymer containing 2,4-dichlorophenoxy for enhanced oil recovery†

Shaohua Gou,<sup>a,b</sup> Yang He,<sup>b</sup> Lihua Zhou,<sup>c</sup> Peng Zhao,<sup>b</sup> Qin Zhang,<sup>b</sup> Shiwei Li<sup>b</sup> and Qipeng Guo<sup>\*d</sup>

We report here a novel anti-biodegradable hydrophobic acrylamide copolymer that was prepared from acrylamide, acrylic acid, sodium 3-(allyloxy)-2-hydroxypropane-1-sulfonate and *N*-allyl-2-(2,4-dichlorophenoxy) acetamide using the 2,2'-azobis(2-methylpropionamide) dihydrochloride initiation system. Subsequently, the copolymer was characterized by FT-IR, <sup>1</sup>H NMR, TG-DTG and water-solubility. And the biodegradability test indicated that the copolymer was not deemed to be readily biodegradable via a closed bottle test established by the Organization for Economic Co-operation and Development (OECD 301 D). Meanwhile the copolymer could significantly enhance the viscosity of the aqueous solution in comparison with partially hydrolyzed polyacrylamide. A viscosity retention of 51.9% indicated the result of a dramatic improvement of temperature tolerance. And then the excellent salt resistance, shear resistance, viscoelasticity, long-term stability of the copolymer could be obtained, which provides a good theoretical foundation for the application in enhanced oil recovery. In addition, this copolymer exerted stronger mobility control ability with a resistance factor of 22.1 and a residual resistance factor of 5.0, and superior ability for enhanced oil recovery of 12.9%. Hence, the copolymer has potential application for enhanced oil recovery in high-temperature and high-salinity reservoirs.

Received (in Montpellier, France)  
13th July 2015,  
Accepted 15th September 2015

DOI: 10.1039/c5nj01821h

www.rsc.org/njc

## Introduction

As an important global energy, petroleum holds a significant position in the development of national economy.<sup>1</sup> Many countries around the world, such as America, Russia, and Arab countries, are rich in oil. However, many oil fields in China have entered the development phase of high water cut. Thereby, a set of perfect enhanced oil recovery (EOR) technologies has been formed due to the enormous petroleum consumption.<sup>2,3</sup> Among these, the application of polymer flooding has achieved approving results.<sup>4–7</sup> For polymer flooding, the viscosity and long-term stability of displacing fluid are not only two of the

important indexes but also two key factors of polymer flooding effectiveness, because polymer flooding technology is mainly to enhance oil recovery by increasing the swept volume and oil displacement efficiency of displacing fluid.<sup>8–11</sup> However, the commonly used EOR chemicals, partially hydrolyzed polyacrylamide (HPAM) and xanthan gum, are difficult to completely meet the factor at high-temperature and under high-salinity conditions due to the hydrolysis, biodegradation, poor ability of increasing viscosity, and others.<sup>12,13</sup> Therefore, the development of some new HPAM substitutes has played an important role in the research of the polymer flooding.<sup>4,14</sup>

Considerable research studies have focused on the ways to improve the resistance of the polymers to the harsh conditions, such as increasing the rigidity of the polymer, and strengthening intermolecular forces.<sup>15–19</sup> McCormick and Bock *et al.* synthesized hydrophobically associating polyacrylamides and examined the effect of temperature and salt on the viscosity of the polymers.<sup>20,21</sup> Additionally, the polymers containing hydrophobic and rigid ring groups exhibit obvious thickening ability, and temperature-thickening properties.<sup>22,23</sup> Therefore, a number of hydrophobically associating polymers have been studied as candidates for enhanced oil recovery. However, the poor solubility has become the limit for their wide application in oil exploration. As we know, strong hydrate groups, such as sulfonic

<sup>a</sup> State Key Laboratory of Oil and Gas Reservoir Geology and Exploitation, Southwest Petroleum University, Chengdu, Sichuan 610500, China.  
E-mail: shaohuagou@swpu.edu.cn

<sup>b</sup> Oil & Gas Field Applied Chemistry Key Laboratory of Sichuan Province, College of Chemistry and Chemical Engineering, Southwest Petroleum University, Chengdu, Sichuan 610500, China

<sup>c</sup> State Key Laboratory of Biotherapy, West China Hospital of Sichuan University, Chengdu, Sichuan 610041, China

<sup>d</sup> Polymers Research Group, Institute for Frontier Materials, Deakin University, Locked Bag 20000, Geelong, Victoria 3220, Australia. E-mail: qguo@deakin.edu.au

† Electronic supplementary information (ESI) available: Optimum copolymerization conditions; intrinsic viscosity of copolymers. See DOI: 10.1039/c5nj01821h

and hydroxyl groups, can significantly improve the water-solubility of the polymers.<sup>24,25</sup> In this paper, sodium 3-(allyloxy)-2-hydroxypropane-1-sulfonate (APS) as a functional monomer was introduced into the polymer chain to enhance the water solubility.

In addition, because a number of bacteria survive in the formation water, commonly used acrylamide copolymers and xanthan gum are vulnerable to be degraded by natural microorganisms. The excellent result for EOR is hard to be obtained when using ordinary polymers. Bao *et al.* found that the HPAM removal efficiency of 36.3% was obtained within the 7 d period when HPAM served as a sole nitrogen source.<sup>26</sup> It was reported that chlorobenzene derivatives were relatively difficult to be degraded by general microorganisms and they can be degraded by only a handful of microorganisms, such as *Pseudomonas* sp. and *Flavobacterium*. Wang *et al.* reported that an average degradation of 5.5% of 1,3-dichlorobenzene by adapting bacterium PF-11 was monitored every day.<sup>27–30</sup> And the introduction of chlorobenzene groups into copolymers could improve their thermal stability and enhance the rigidity of the copolymers.<sup>31–34</sup> In this work, *N*-allyl-2-(2,4-dichlorophenoxy)acetamide (DCAP) as a functionalized hydrophobic monomer was copolymerized with sodium 3-(allyloxy)-2-hydroxypropane-1-sulfonate (APS), acrylamide (AM) and acrylic acid (AA). This water-soluble hydrophobic copolymer was investigated systematically on several aspects such as water solubility, biodegradability, thickening properties, salt resistance, rheological properties, and EOR ability, which provides a theoretical basis for its potential application as a new EOR chemical.

## Experimental

### Materials

The chemicals, acrylamide (AM), acrylic acid (AA), 2,2'-azobis-(2-methylpropionamide) dihydrochloride (V-50), alkylphenol ethoxylates (OP-10), 2-(2,4-dichlorophenoxy) acetic acid, triethylamine, thionyl chloride, CH<sub>2</sub>Cl<sub>2</sub>, NaOH, NaCl, MgCl<sub>2</sub>·6H<sub>2</sub>O, CaCl<sub>2</sub>, NaSO<sub>3</sub>, were of analytical purity and purchased from Chengdu Kelong Chemical Reagent Factory Co. (Sichuan, China). Allylamine was purchased from Nanjing Forward Chemical Reagent Factory Co. (Nanjing, China). 1-Allyloxy-2,3-epoxy propane was supplied by Qufu Huarong New Chemical Materials Co., Ltd (Shandong, China). HPAM ( $M_n = 6.5 \times 10^6$ ) was obtained from Daqing Refining and Chemical Company. Other chemicals were commercially available and used directly without further purification.

### Synthesis of APS and DCAP

Sodium 3-(allyloxy)-2-hydroxypropane-1-sulfonate (APS) was synthesized according to the method reported by the literature, and the synthesis route was shown in Scheme S1a (see ESI<sup>†</sup>).<sup>35</sup> *N*-allyl-2-(2,4-dichlorophenoxy)acetamide (DCAP) was obtained using 2-(2,4-dichlorophenoxy)acetic acid, thionyl chloride and allylamine as raw materials, as shown in Scheme S1b (see ESI<sup>†</sup>). 2-(2,4-dichlorophenoxy)acetic acid (2a) (0.10 mol) was completely dissolved with 30 mL CH<sub>2</sub>Cl<sub>2</sub> in a 250 mL round bottom flask, and then thionyl chloride (0.12 mol) was slowly added within

30 min. The reaction was carried out under reflux at 55 °C for 4 h. Then the mixture was cooled to room temperature. The solvent and excessive thionyl chloride were removed by rotary evaporation, 2-(2,4-dichlorophenoxy)acetyl chloride (2b) was obtained. All of 1c was dissolved in a 50 mL round bottom flask with 15 mL CH<sub>2</sub>Cl<sub>2</sub>. In an ice bath, allylamine (0.11 mol) and triethylamine (0.15 mol) dissolved in 10 mL CH<sub>2</sub>Cl<sub>2</sub> were slowly added with intense stirring for 5 h. Then the mixture was successively washed by deionized water, dilute hydrochloric acid, and saturated salt solution, dried using anhydrous sodium sulfate, evaporated. Then light yellow solid *N*-allyl-2-(2,4-dichlorophenoxy)acetamide (DCAP, 83.4% yield) was obtained. The <sup>1</sup>H NMR and <sup>13</sup>C NMR spectra of DCAP were displayed in Fig. S1 (see ESI<sup>†</sup>). DCAP: <sup>1</sup>H NMR (400 MHz, CDCl<sub>3</sub>, δ, ppm): 4.0 (s, 2H, -CH<sub>2</sub>-NH-), 4.5 (s, 2H, -C(O)-CH<sub>2</sub>-O-), 5.2–5.3 (dd,  $J_1 = 17.3$  Hz,  $J_2 = 10.4$  Hz, 2H, CH<sub>2</sub>-HC = CH<sub>2</sub>), 5.9 (m, 1H, H<sub>2</sub>C = CH-CH<sub>2</sub>-), 6.9 (t,  $J_1 = 4.9$  Hz,  $J_2 = 2.8$  Hz, 2H, Ar-5'-H, Ar-6'-H), 7.2 (dd,  $J_1 = 2.8$  Hz,  $J_2 = 4.0$  Hz, 1H, Ar-3'-H), 7.4 (s, 1H, N-H); <sup>13</sup>C NMR (100 MHz, CDCl<sub>3</sub>, δ, ppm): 41.3, 68.4, 114.7, 116.6, 123.8, 127.5, 128.0, 130.2, 133.5, 151.6, 166.9.

### Synthesis of AM/AA/APS and AM/AA/APS/DCAP

AM/AA/APS and AM/AA/APS/DCAP were prepared by AM, AA, APS and DCAP using a V-50 initiator system (for details, see ESI<sup>†</sup>), as shown in Scheme 1. Briefly, all the monomers with appropriate composition were dissolved in deionized water. Additionally, for AM/AA/APS/DCAP, OP-10 was added as a solubilizing agent. The pH of the reaction system was adjusted by NaOH solution. The initiator V-50 was added into reaction system under a nitrogen atmosphere at indicated temperature. After reacting for 8 h, the copolymer gels were washed with ethanol, and then dried at 40 °C in a vacuum for 24 h to obtain the corresponding copolymers, AM/AA/APS and AM/AA/APS/DCAP.

### Characterization

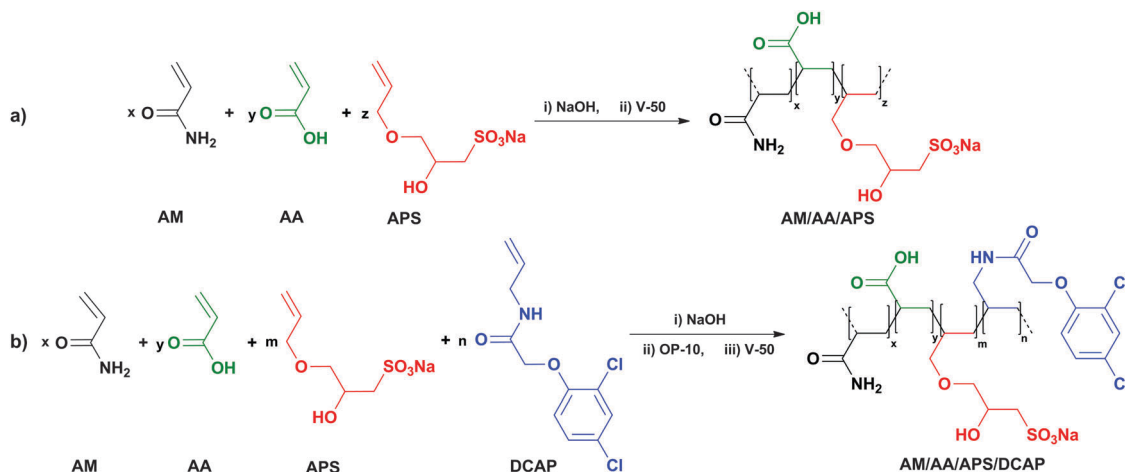
**Gel permeation chromatography (GPC).** The molecular weights of AM/AA/APS and AM/AA/APS/DCAP with a concentration of 100 mg L<sup>-1</sup> were measured using Waters E2695 Gel Permeation Chromatography (Waters, America) at 30 °C using NaNO<sub>3</sub> aqueous solution (1.0 M) as an eluent. The flow rate was 1.0 mL min<sup>-1</sup>.

**Elemental analysis.** The elemental analysis of AM/AA/APS and AM/AA/APS/DCAP was carried out using a Vario EL-III elemental analyzer (Elementar, Germany).

**Fourier transform infrared (FT-IR) spectroscopy.** The FT-IR spectra of AM/AA/APS and AM/AA/APS/DCAP were obtained using a WQF-520A Fourier Transform Infrared spectrophotometer (Beijing Beifen-Ruili Analytical Instrument Co., Ltd, China) with KBr pellets by averaging 32 scans at room temperature.

**<sup>1</sup>H nuclear magnetic resonance (<sup>1</sup>H NMR) spectroscopy.** The <sup>1</sup>H NMR spectra of AM/AA/APS and AM/AA/APS/DCAP were recorded on a Bruker AVANCE III 400 MHz NMR spectrometer (Bruker, Switzerland) in D<sub>2</sub>O.

**Intrinsic viscosity measurements.** The flux time of copolymer solution of different concentrations with 1 mol L<sup>-1</sup> NaCl was



Scheme 1 (a) The synthesis route of AM/AA/APS, (b) the synthesis route of AM/AA/APS/DCAP.

measured using an Ubbelohde viscometer at 30 °C. The specific viscosity ( $\eta_{sp}$ ) and intrinsic viscosity  $[\eta]$  were calculated using the following eqn (1) and (2).<sup>36</sup>

$$\eta_{sp} = \frac{t - t_0}{t_0} \quad (1)$$

$$[\eta] = \lim_{C \rightarrow 0} \eta_{sp} / C \quad (2)$$

in which  $\eta_{sp}$  is the specific viscosity of the copolymer;  $t_0$  is the flux time of 1 mol L<sup>-1</sup> NaCl solution,  $s$ ; and  $t$  is the flux time of copolymer brine solution,  $s$ .

As shown in Fig. S4 (see ESI<sup>†</sup>), the results revealed that  $[\eta]$  of AM/AA/APS and AM/AA/APS/DCAP was 1326 mL g<sup>-1</sup> and 1317 mL g<sup>-1</sup>, respectively.

**Thermogravimetry and derivative thermogravimetry (TG-DTG).** In a nitrogen atmosphere (flow rate: 50 mL min<sup>-1</sup>), 7.0305 mg AM/AA/APS and 7.1900 mg AM/AA/APS/DCAP were tested using a TGA/SDTA851e Thermogravimetric and Differential Thermal Analyzer (METTLER TOLEDO Co., Switzerland) from 25 to 800 °C at 10 °C min<sup>-1</sup>, and then the TG and DTG curves were obtained to analyze the thermal stability of the copolymers.

### Water solubility

Copolymer particles (40–45 meshes, 2000 mg) were dissolved in 1000 mL deionized water, recording solution conductivity. The solution conductivity was measured by using a DDS-11A conductivity meter (Shanghai Rex Xinjing Instrument Co., Ltd, China). Dissolution time is defined as the time from adding the copolymer to solution conductivity stabilizing.<sup>37</sup>

### Biodegradability test

Biodegradability of AM/AA/APS, AM/AA/APS/DCAP, HPAM and xanthan gum was obtained from biochemical oxygen demand (BOD) and chemical oxygen demand (COD) using the closed bottle test (OECD 301 D).<sup>38–40</sup> Briefly, the mixture of the copolymer (3.0 mg L<sup>-1</sup>), as a sole carbon source, and the secondary effluent was, respectively, added into the same BOD

bottles. All the bottles were maintained in full and then incubated in dark at 20 °C for 28 days. The dissolved oxygen of each BOD bottles was measured using a DO-200 dissolved oxygen analyzer (Nanjing Zhuoma electromechanical Co. Ltd, China), and then the remaining BOD bottles continued to be cultured under the same conditions. The COD was determined using the potassium dichromate reflux method. The degradation rate ( $D_t$ ) is obtained at frequent intervals over a 28 d period by the following eqn (3).

$$D_t(\%) = \frac{\text{BOD}(\text{O}_2 \text{ mg}/\text{test substance mg})}{\text{COD}(\text{O}_2 \text{ mg}/\text{test substance mg})} \times 100 \quad (3)$$

### Tackifying and salt tolerance

Tackifying of copolymers was investigated by measuring the apparent viscosity of different concentration of the copolymer solutions. Copolymer solutions with a salt tolerance of 2000 mg L<sup>-1</sup> were investigated at different concentrations of small molecule electrolytes, such as NaCl, MgCl<sub>2</sub>, and CaCl<sub>2</sub>. The apparent viscosities of the copolymer solutions were determined using a Brookfield DV-III Programmable Rheometer (Brookfield Co., America) with a 00<sup>#</sup> (6 rpm) or 62<sup>#</sup> (18.8 rpm) rotor.

### Rheological measurements

Temperature resistance of the copolymer solution with 2000 mg L<sup>-1</sup> was measured using a HAAKE MARS III rheometer (HAAKE, Germany) from 20 to 120 °C at 7.34 s<sup>-1</sup>.

Shear thinning behavior of the copolymer solution with 2000 mg L<sup>-1</sup> was investigated on a HAAKE MARS III rheometer (HAAKE, Germany) from 7.34 to 1000 s<sup>-1</sup> at 25 °C.

Shear resistance of the copolymer solution with 2000 mg L<sup>-1</sup> was studied on a HAAKE MARS III rheometer (HAAKE, Germany) at 25 °C. The copolymer solution was measured at 7.34 s<sup>-1</sup>, 1000 s<sup>-1</sup>, and 7.34 s<sup>-1</sup> for 30 min, respectively.

Viscoelasticity of the copolymer solution with 2000 mg L<sup>-1</sup> was obtained by measuring the elastic modulus and viscous modulus of the copolymer solution in the frequency scanning range, 0.01–10 Hz.

**Table 1** Composition and content of the total dissolved solid in the simulated formation water

Inorganic ions	Na <sup>+</sup>	Mg <sup>2+</sup>	Ca <sup>2+</sup>	Cl <sup>-</sup>	SO <sub>4</sub> <sup>2-</sup>	HCO <sub>3</sub> <sup>-</sup>	CO <sub>3</sub> <sup>2-</sup>	TDS
Content (mg L <sup>-1</sup> )	6588	348	435	10 883	1004	126	205	19 589

### Long-term stability

2000 mg copolymers with long-term stability dissolved in 1.0 L simulated formation water were investigated by measuring the apparent viscosity of the solution at different times at 80 °C for 60 days on a Brookfield DV-III Programmable Rheometer (Brookfield Co., America) with a 00<sup>#</sup> (6 rpm) or 62<sup>#</sup> (18.8 rpm) rotor. And the content and composition of the total dissolved solid (TDS) in simulated formation water were listed in Table 1.

### Mobility control analysis

Mobility control ability of the copolymer solutions with 2000 mg L<sup>-1</sup> was characterized by the resistance factor (RF) and the residual resistance factor (RRF).<sup>41,42</sup> The core barrel with a length of 250 mm and an internal diameter of 25 mm was packed with quartz sand which was washed by hydrochloric acid and distilled water several times. The copolymers were dissolved in simulated formation water (Table 1). Core flow experiments were carried out at 80 °C in an incubator. The injection pressure was recorded using a pressure sensor. The infection rate of water saturation, copolymer solution and water flooding was 2.0 mL min<sup>-1</sup> measured using an ISCO 260D syringe pump. The RF and RRF were calculated by the following eqn (4) and (5).

$$RF = \frac{P_p/Q_p}{P_{ws}/Q_{ws}} \quad (4)$$

$$RRF = \frac{P_{wf}/Q_{wf}}{P_{ws}/Q_{ws}} \quad (5)$$

in which  $P_p$  is the stable pressure when injecting copolymer solution, MPa;  $Q_p$  is the injecting rate when injecting the copolymer solution, mL min<sup>-1</sup>;  $P_{ws}$  is the stable pressure when saturating water, MPa; and  $Q_{ws}$  is the injecting rate when saturating water, mL min<sup>-1</sup>;  $P_{wf}$  is the stable pressure when water flooding, MPa; and  $Q_{wf}$  is the injecting rate when water flooding, mL min<sup>-1</sup>.

### Enhanced oil recovery analysis

EOR ability of the copolymer solutions with 2000 mg L<sup>-1</sup> was investigated *via* core flooding experiments at 80 °C. The core was saturated and aged with crude oil for 2 days. The core was flooded with simulated formation water at 0.2 mL min<sup>-1</sup> until the water cut was up to 95%; the copolymer solution of 0.3 time

pore volume (PV) was injected. The EOR value was obtained by the following eqn (6).

$$EOR = H_t - H_w \quad (6)$$

in which EOR is the enhanced oil recovery, %;  $H_t$  is the oil recovery of the whole displacement process, %; and  $H_w$  is the oil recovery of water flooding, %.

## Results and discussion

### Synthesis of AM/AA/APS and AM/AA/APS/DCAP copolymers

The copolymers AM/AA/APS and AM/AA/APS/DCAP were synthesized through copolymerization of AM, AA, APS and DCAP. The compositions of copolymers AM/AA/APS were obtained by elemental analysis. And the composition of AM/AA/APS/DCAP was determined by <sup>1</sup>H NMR and elemental analysis (see ESI†). The molecular weights of AM/AA/APS and AM/AA/APS/DCAP were measured by GPC. The results are listed in Table 2.

Fig. 1a shows the FT-IR spectra of AM/AA/APS and AM/AA/APS/DCAP copolymers. For AM/AA/APS, the peaks at 3406 cm<sup>-1</sup> and 3181 cm<sup>-1</sup> were the stretching vibration peaks of N-H. The stretching vibration peak of C-H was at 2928 cm<sup>-1</sup>. The peak at 1674 cm<sup>-1</sup> was assigned to the characteristic peak of C=O. The peaks at 1197 cm<sup>-1</sup> and 1042 cm<sup>-1</sup> were the characteristic absorption peaks of -SO<sub>3</sub>Na. The stretching vibration of C-O-C was the peak at 1114 cm<sup>-1</sup>. The result indicated that AM, AA, and APS were copolymerized to the chain of the copolymer. For the FT-IR spectra of AM/AA/APS/DCAP, the characteristic absorption peaks of N-H, C-H, C=O, C-O-C, and -SO<sub>3</sub>Na groups existed in the corresponding location that were similar to the FT-IR spectra of AM/AA/APS. Additionally, two weak absorption peaks at 879 cm<sup>-1</sup> and 816 cm<sup>-1</sup> could be observed, which were attributed to the characteristic peaks of 1,2,4-trisubstituted benzene groups. It has been found the successful copolymerization of AM, AA, APS, and DCAP.

The <sup>1</sup>H NMR spectrum of AM/AA/APS/DCAP was shown in Fig. 1b. It was obvious that the protons of the aliphatic -CH<sub>2</sub>- group of the main copolymer chain appeared at 1.59–1.71 ppm. The chemical shift value at 2.15–2.26 ppm was related to the protons of -CH- in the main copolymer chain. The signal of protons at 2.37 ppm showed the existence of -CH<sub>2</sub>-NH-CO- groups. The signal of protons at 2.50 ppm was due to -CH<sub>2</sub>-O-CH<sub>2</sub>-CH(OH)- groups. The characteristic peak at 3.12 ppm was assigned to the protons of [-O-CH<sub>2</sub>-CH(OH)-CH<sub>2</sub>-] groups. The signal of protons was observed at 3.47 ppm due to -CH<sub>2</sub>- of [-CH(OH)-CH<sub>2</sub>-SO<sub>3</sub>Na] groups. The signal of protons of -CH<sub>2</sub>-CH(OH)-CH<sub>2</sub>- appeared at 3.76 ppm. The chemical shift at 3.84 ppm was assigned to the protons of -NH-CO-CH<sub>2</sub>-O- groups.

**Table 2** Compositions and molecular weights of AM/AA/APS and AM/AA/APS/DCAP copolymers

Copolymer	Molar ratio of reactants (%)				Elements mass ratio (%)			Molar composition of copolymer (%)				$M_w (\times 10^6)$	$M_w/M_n$
	AM	AA	APS	DCAP	C	N	S	AM	AA	APS	DCAP		
AM/AA/APS/DCAP	82.55	15.46	1.70	0.29	47.26	14.59	0.65	80.93	17.25	1.57	0.25	6.51	2.12
AM/AA/APS	82.79	15.50	1.71	—	47.21	15.00	0.69	83.06	15.26	1.68	—	6.69	2.03

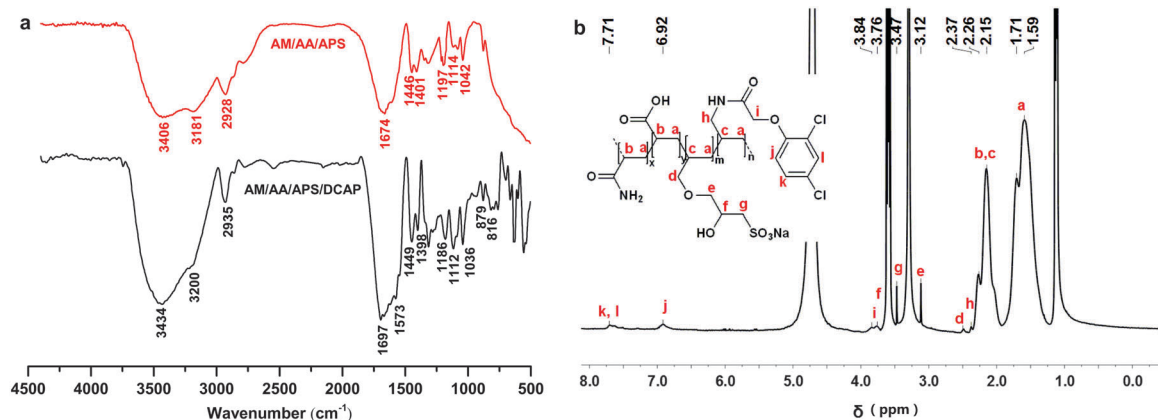


Fig. 1 (a) IR spectra of AM/AA/APS and AM/AA/APS/DCAP, (b)  $^1\text{H}$  NMR spectra of AM/AA/APS and AM/AA/APS/DCAP.

And the signal of protons at 6.92 ppm and 7.71 ppm exhibited the presence of the protons in the benzene ring.

### Water solubility

The introduction of hydrophobic monomers can significantly affect water solubility of the copolymer. Therefore, the dissolution time of AM/AA/APS, AM/AA/APS/DCAP and HPAM was determined to investigate the water solubility of the copolymers, as shown in Fig. 2a. It was found that the dissolubility curves of three copolymers displayed a similar trend. The results indicated that the complete dissolution of AM/AA/APS/DCAP just needed an extra 15 min compared with HPAM (84 min). The dissolubility of hydrophobic copolymers was significantly improved by introducing strong hydrate groups, sulfonic and hydroxyl groups, which could be found from the result of the

dissolubility of AM/AA/APS with a short dissolution time of 73 min. The hydrophobic copolymer AM/AA/APS/DCAP had excellent water solubility as expected.

### Biodegradability

Biodegradability of AM/AA/APS/DCAP, AM/AA/APS, HPAM and xanthan gum was analysed *via* a degradation rate ( $D_t$ ), as displayed in Fig. 2b. From the comparative degradation study, it has been observed that xanthan gum, AM/AA/APS and HPAM showed rapid degradation within a 16 d period, and then reached a plateau. It was obvious that xanthan gum, AM/AA/APS and HPAM exhibited an accelerated rate of degradation than AM/AA/APS/DCAP. Refer to the standard 301 established by the Organization for Economic Co-operation and Development (OECD), the degradation which reaches the pass level of 60% is considered to be as “ready biodegradability”. As shown in Fig. 2b, the degradation of xanthan gum, AM/AA/APS and HPAM had been reached 60% within the 28 d period of the test. The degradation rate of AM/AA/APS/DCAP was far less than 60%, which indicated that the degradation could be minimized by the incorporation of 2,4-dichlorophenoxy and AM/AA/APS/DCAP was less susceptible to biodegradability.

### Effects of concentration on the apparent viscosity

Tackifying, as one of the most important copolymer properties, was investigated by measuring the apparent viscosity of AM/AA/APS, AM/AA/APS/DCAP, and HPAM solution at concentration, 100–3000 mg L<sup>-1</sup>. It was clear from Fig. 3 that the apparent viscosity of AM/AA/APS and HPAM solution displayed a linear growth with an increase of the copolymer concentration. Unlike AM/AA/APS and HPAM, a slow increase in apparent viscosity at a concentration from 100 to 800 mg L<sup>-1</sup> was observed for AM/AA/APS/DCAP, which might be explained by the coil of the polymer chain as the result of intramolecular association of 2,4-dichlorophenoxy groups at low copolymer concentration. However, AM/AA/APS/DCAP displayed a rapid growth in apparent viscosity above 800 mg L<sup>-1</sup> copolymer solution. With an increase of the solution concentration, the three-dimensional network formed due to hydrophobic association among the polymer chain

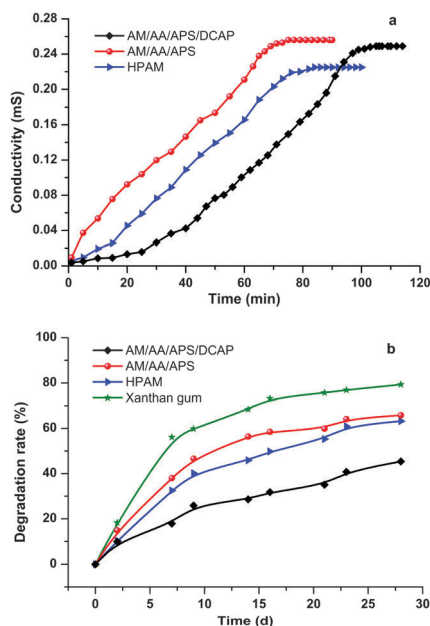


Fig. 2 (a) Dissolution time curves of HPAM, AM/AA/APS and AM/AA/APS/DCAP, (b) biodegradability of HPAM, AM/AA/APS, AM/AA/APS/DCAP and xanthan gum.

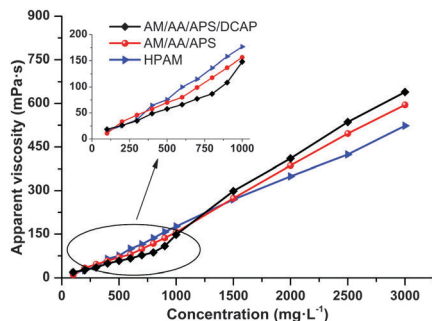


Fig. 3 Tackifying of HPAM, AM/AA/APS and AM/AA/APS/DCAP.

can contribute to the rapid increase in apparent viscosity.<sup>43</sup> Therefore, from 800 to 900 mg L<sup>-1</sup>, AM/AA/APS/DCAP exhibited a sharp increase in apparent viscosity of copolymer solution. As shown in Fig. 3, AM/AA/APS/DCAP exhibited a higher apparent viscosity of 410.5 mPa s than that of AM/AA/APS (386.7 mPa s) and HPAM (349.4 mPa s) at a concentration of 2000 mg L<sup>-1</sup>, which revealed that AM/AA/APS/DCAP possessed better thickening ability.

### Effects of salt on the apparent viscosity

Salt tolerance, as another important performance, was investigated because of the existence of various inorganic ions in the formation water. The apparent viscosity as a function of NaCl, CaCl<sub>2</sub>, and MgCl<sub>2</sub> was usually studied to obtain salt tolerance of the copolymer.<sup>44</sup> The results are shown in Fig. 4. For three copolymers, a first decrease, and then a stationary trend in apparent viscosity were observed when adding NaCl, CaCl<sub>2</sub>, and MgCl<sub>2</sub> into the copolymer solution. In deionized water, an extended state of the polymer chain contributes to the high apparent viscosity due to the electrostatic repulsion of -COO<sup>-</sup>. Adding a small molecule electrolyte can lead to the coil of the polymer chain because of the electrostatic shielding, which showed relatively low apparent viscosity. However, in comparison with HPAM solution, the stable viscosity of AM/AA/APS was higher than HPAM because of the introduction of a strong hydrate group and a sulfonate group. In addition, AM/AA/APS/DCAP had a higher value of apparent viscosity than AM/AA/APS and HPAM, which was ascribed to hydrophobic 2,4-dichlorophenoxy and sulfonate groups.<sup>45</sup> It has also been found that the effect of divalent cations on apparent viscosity of the copolymer solution was greater than that of monovalent cations.

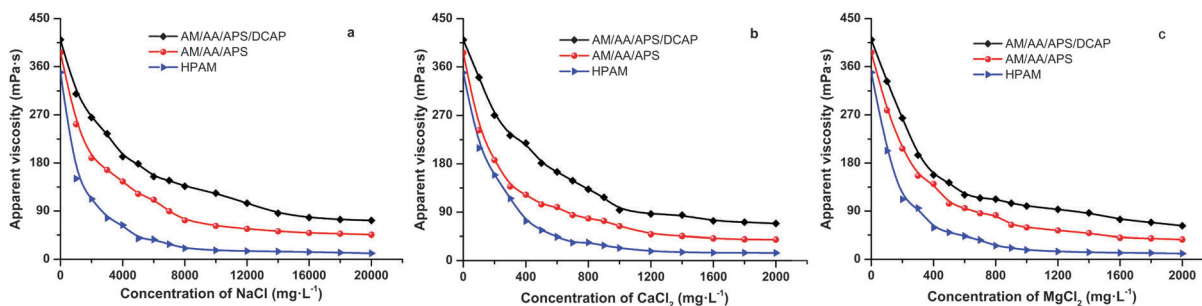


Fig. 4 NaCl, CaCl<sub>2</sub> and MgCl<sub>2</sub> tolerance of AM/AA/APS, AM/AA/APS/DCAP and HPAM solution.

As shown in Fig. 4a, the viscosity rate of AM/AA/APS/DCAP, AM/AA/APS, and HPAM solution with 20 000 mg L<sup>-1</sup> NaCl was 17.6%, 11.8%, and 3.2%, respectively. And the copolymers with 2000 mg L<sup>-1</sup> CaCl<sub>2</sub> exhibited a slightly low viscosity retention rate (AM/AA/APS/DCAP: 16.7%, AM/AA/APS: 10.1%, and HPAM: 4.1%) as shown in Fig. 4b. A similar change tendency of the apparent viscosity of the copolymers with 2000 mg L<sup>-1</sup> MgCl<sub>2</sub> was observed in Fig. 4c, which showed that the viscosity retention rate of AM/AA/APS/DCAP, AM/AA/APS, and HPAM was 15.2%, 9.3% and 3.1%, respectively.

### Thermal stability

The thermal stability of the copolymers, AM/AA/APS and AM/AA/APS/DCAP, was investigated as shown in Fig. 5. It was found that the TG curve of AM/AA/APS displayed three stages in Fig. 5a. The copolymer lost 8.18% of its mass in the range of 25–176 °C, which was due to the loss of free water and bound water present in the copolymer sample. The second process occurred in the range of 176–431 °C, with a mass loss of 50.64%. Meanwhile, there were three peaks of the weight loss rate appearing at 205, 225 and 323 °C in the DTG curve. At this stage, the reduction of the copolymer's mass was mainly due to breaking up of the polar bonds (C–O, C–H and C–N bonds) and decomposition of sulfonate groups in the side chains. The third step took place beyond 431 °C with the mass loss of 33.53%, which was believed to be associated with the breakage of the C–C bonds in the AM/AA/APS chain.<sup>46,47</sup>

As shown in Fig. 5b, the TG curve of AM/AA/APS/DCAP exhibited three similar stages with AM/AA/APS of a mass loss of 5.79% at 25–176 °C, a mass loss of 64.01% in the range of 176–482 °C and a mass loss of 19.90% beyond 482 °C. What is more, the position and strength of the weight loss rate peaks in the DTG curve of AM/AA/APS/DCAP at the second stage were essentially identical to AM/AA/APS. An additional peak at 445 °C was observed in the DTG curve of AM/AA/APS/DCAP, which might be the extraction of 2,4-dichlorophenoxy groups. The residual mass of AM/AA/APS/DCAP (10.30%) at 800 °C was more than that of AM/AA/APS (7.65%). The result indicated that the AM/AA/APS/DCAP copolymer had excellent thermal stability.

### Effects of temperature on the apparent viscosity

The thermal stability of AM/AA/APS, AM/AA/APS/DCAP, and HPAM solution was investigated by measuring the change of

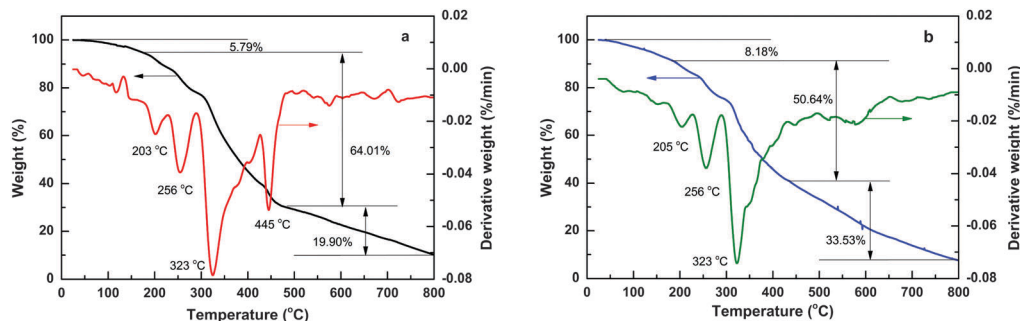


Fig. 5 TG-DTG curves of (a) AM/AA/APS/DCAP and (b) AM/AA/APS.

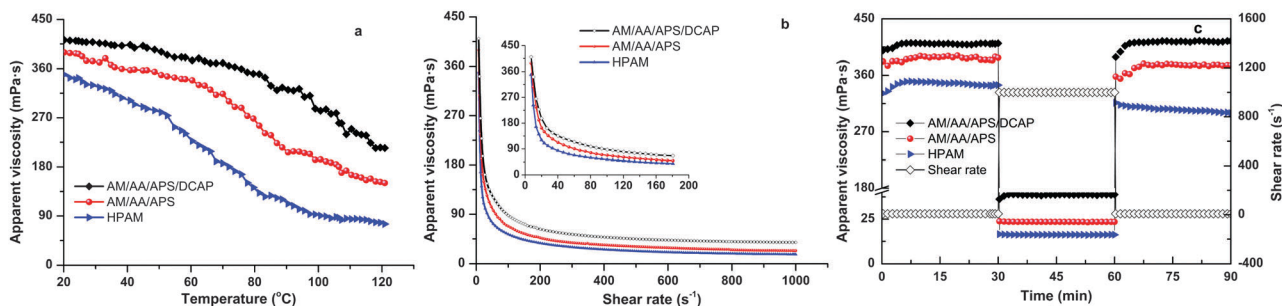


Fig. 6 (a) Temperature resistance of the copolymers, (b) shear thinning behavior of the copolymers, (c) shear recovery of the copolymers.

the apparent viscosity from 20 °C to 120 °C. The change in trend was displayed in Fig. 6a. A significant decrease in apparent viscosity was observed as the temperature increased, and the viscosity retention rate of 21.5% at 120 °C was relatively low compared to that at 25 °C for HPAM solution. The apparent viscosity of AM/AA/APS/DCAP and AM/AA/APS showed a slight variation at low temperature and then a large reduction at high temperature. However, the apparent viscosity of AM/AA/APS/DCAP decreased significantly from 85 °C, and the temperature at which the apparent viscosity of the copolymer solution began to reduce sharply was distinctly higher than that of AM/AA/APS. The high viscosity retention obtained, 51.9%, indicated the extraordinary temperature resistance at 120 °C, which was ascribed to the strong hydration ability of sulfonate groups and the strong interaction among hydrophobic groups within the temperature range.<sup>48,49</sup>

### Effects of shear on the apparent viscosity

**Shear thinning behavior.** The effect of shear rate on the apparent viscosity of the copolymers was studied, as illustrated in Fig. 6b. It was found that AM/AA/APS/DCAP, AM/AA/APS and HPAM solutions revealed non-Newtonian shear-thinning behavior. As the shear rate increased from 7.34 to 100 s<sup>-1</sup>, the viscosity of copolymer solutions dropped obviously, and then the viscosity maintained a small decreasing trend within the shear rate range. However, because of the introduction of rigid groups, 2,4-dichlorophenoxy, the higher viscosity retention value of AM/AA/APS/DCAP, 9.4%, could be obtained as the shear rate changed from 7.34 to 1000 s<sup>-1</sup> in comparison with AM/AA/APS (6.0%) and HPAM (4.7%).

**Shear recovery behavior.** The shear recovery behavior was investigated because a long time interaction of high shear is easy to destroy the molecular structure of the polymer when displacing fluid was injected into the formation. As exhibited in Fig. 6c, it was evident that the apparent viscosity of AM/AA/APS/DCAP returned to the initial value after 30 min shear at 1000 s<sup>-1</sup>. For AM/AA/APS, a low viscosity loss, 3.0%, was observed under 1000 s<sup>-1</sup>. However, the apparent viscosity of HPAM decreased obviously after 30 min shear at 1000 s<sup>-1</sup>, and exhibited a loss of 12.9%. The results indicated that AM/AA/APS/DCAP possessed fantastic shear resistance due to the introduction of rigid groups.

### Viscoelasticity

The viscoelasticity of AM/AA/APS/DCAP, AM/AA/APS, and HPAM solutions was researched by the obtained viscous modulus ( $G''$ ) and elastic modulus ( $G'$ ), as shown in Fig. 7a. It could be seen from Fig. 7a that both  $G''$  and  $G'$  increased gradually within the oscillation frequency range. Both  $G''$  and  $G'$  of AM/AA/APS/DCAP and AM/AA/APS were significantly higher than those of HPAM. As shown in Fig. 7a,  $G'$  of HPAM surpassed its  $G''$  at a high frequency (> 1.0 Hz), which indicated that HPAM exerted the elastic properties. The elasticity of AM/AA/APS was greater than viscosity at a low frequency of 0.2 Hz. While AM/AA/APS/DCAP showed distinct elastic behavior within the scan frequency range, which was mainly due to enhanced rigidity of the copolymer.<sup>50</sup> The excellent viscoelasticity, especially elasticity, might contribute to improving the swept area of displacing fluid to enhance oil recovery in a porous medium.<sup>51</sup>

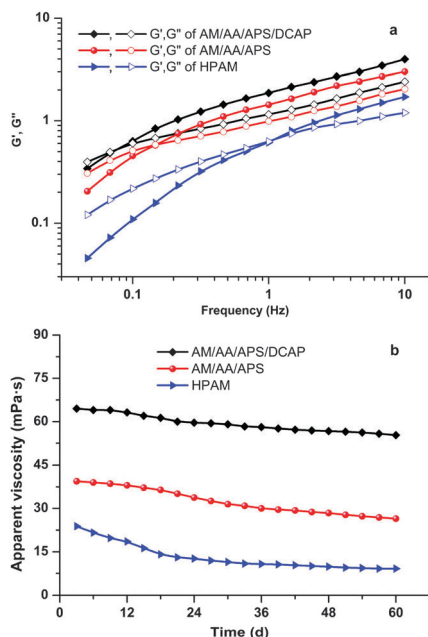


Fig. 7 (a) Viscoelastic behavior of the copolymers, (b) long-term stability of the copolymers.

### Long-term stability

The long-term stability is significantly important for displacing fluid that flows in formation for a long time. As shown in Fig. 7b, the apparent viscosity as a function of time was investigated under the condition of seal. All the copolymers exhibited a slight reduction in apparent viscosity, and the loss in apparent viscosity of HPAM, 38.2%, was larger than that of AM/AA/APS/DCAP and AM/AA/APS. Little viscosity loss was observed for AM/AA/APS/DCAP after sealing for 60 days at 80 °C. The results showed that AM/AA/APS/DCAP possessed remarkable long-term stability.

### Mobility control ability

The flow characteristic behavior of AM/AA/APS/DCAP, AM/AA/APS, and HPAM solutions in porous media was studied *via* core flooding experiments. As seen in Fig. 8a, three evident stages for three copolymers were visible in the injection pressure curves. It was clear that the injection pressure of water saturation was gradually stable until injecting 2.4 PV simulated formation water. Then the injection pressure rose to a large extent along with the increase of injection volume of the copolymer solutions. And the injecting pressure has become relatively stable within the injection volume range from about 5.0 to 8.0 PV. However, the stable pressure of injecting different polymer solution varied enormously on account of various polymers possessing hydrodynamic volume. It could be observed that AM/AA/APS/DCAP exhibited the greatest injection pressure, 0.2427 MPa, in comparison with AM/AA/APS and HPAM. The introduction of hydrophobic 2,4-dichlorophenoxy and sulfonate groups led to the increase of hydrodynamic volume, which made potentially detrimental flow of the copolymers in porous media. Thereby, the greater pressure and larger volume might be needed to

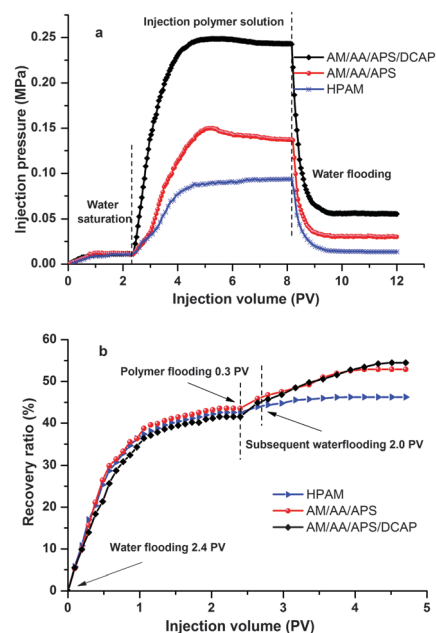


Fig. 8 (a) Mobility control ability of AM/AA/APS/DCAP, AM/AA/APS and HPAM, (b) enhanced oil recovery ability of AM/AA/APS/DCAP, AM/AA/APS and HPAM.

promote the steady flow for the polymers with big hydrodynamic volume. In the process of injecting sequent water, the polymer content in the core became less and less with the more formation water injecting into the core. It was recognized that the pressure declined sharply when injecting sequent water.

As listed in Table 3, all the injection pressure was recorded and the resistance factor (RF) and the residual resistance factor (RRF) were obtained by eqn (4) and (5). It was found the AM/AA/APS/DCAP solution could establish much higher RF of 22.1 and RRF of 5.0 than that of AM/AA/APS (RF: 11.5, RRF: 2.5) and HPAM (RF: 8.9, RRF: 1.3) under the same conditions, which indicated that AM/AA/APS/DCAP solution had stronger mobility control ability that was favourable to enhance oil recovery.

### Enhanced oil recovery

EOE ability of AM/AA/APS/DCAP, AM/AA/APS and HPAM was investigated on the basis of water flooding, as displayed in Fig. 8b. The polymer solution of 0.3 PV was injected into the core to achieve a high recovery ratio after gaining steady recovery, 42.5%, under the condition of water flooding of 2.4 PV. It was found that AM/AA/APS solution could enhance additional recovery of 9.3% compared with HPAM (3.7%). However, the extra recovery

Table 3 RF and RRF of AM/AA/APS/DCAP, AM/AA/APS and HPAM

Polymer	Water saturation pressure ( $10^{-3}$ MPa)	Polymer solution pressure ( $10^{-3}$ MPa)	Water flooding pressure ( $10^{-3}$ MPa)	RF	RRF
AM/AA/APS/DCAP	11.0	242.7	55.4	22.1	5.0
AM/AA/APS	11.9	137.4	30.0	11.5	2.5
HPAM	10.5	93.5	13.6	8.9	1.3

ratio of 12.9% could be obtained when flooding with AM/AA/APS/DCAP solution. The results of core flooding experiments showed that AM/AA/APS/DCAP had superior ability to enhance oil recovery, which was supported by the excellent performance achieved in the previous research studies.

## Conclusions

In conclusion, a hydrophobic acrylamide copolymer was prepared successfully by acrylamide, acrylic acid, sodium 3-(allyloxy)-2-hydroxypropane-1-sulfonate and *N*-allyl-2-(2,4-dichlorophenoxy)acetamide using the 2,2'-azobis(2-methyl propionamide) dihydrochloride system for enhanced oil recovery. The copolymer exhibited excellent performances on water solubility, resistance to biodegradability, and tackifying. It has also been found that the copolymer possessed remarkable salt resistance with a viscosity retention rate of 17.6% under the condition of 20 000 mg L<sup>-1</sup> NaCl, 16.7% under the condition of 2000 mg L<sup>-1</sup> CaCl<sub>2</sub>, and 15.2% under the condition of 2000 mg L<sup>-1</sup> MgCl<sub>2</sub>. And the better temperature tolerance, shear resistance, viscoelasticity, and long-term stability could be obtained compared with partially hydrolyzed polyacrylamide. It was also shown that the copolymer displacing solution had stronger mobility control ability with an RF of 22.1 and an RRF of 5.0, and superior ability to enhance oil recovery of 12.9%. And the further research on the microstructure of the copolymer solution, displacement efficiency under various conditions, and applications of other similar copolymers for EOR chemical is in progress.

## Acknowledgements

This work was supported by the Scientific Research Starting Project of Southwest Petroleum University (contract grant numbers 2014PYZ008 & 2014SJZ759), the Key Programs of Educational Commission of Sichuan Province of China (Natural Science, contract grant number 15ZA0051), the Foundation of Youth Science and Technology Innovation Team of Sichuan Province (contract grant number 2015TD0007).

## References

- 1 S. Sorrell, J. Speirs, R. Bentley, A. Brandt and R. Miller, *Energy Policy*, 2010, **38**, 5290–5295.
- 2 I. Rodríguez-Palmeiro, I. Rodríguez-Escontrela, O. Rodríguez, A. Arce and A. Soto, *RSC Adv.*, 2015, **5**, 37392–37398.
- 3 S. Lago, H. Rodríguez, M. K. Khoshkbarchi, A. Soto and A. Arce, *RSC Adv.*, 2012, **2**, 9392–9397.
- 4 D. A. Z. Wever, F. Picchioni and A. A. Broekhuis, *Prog. Polym. Sci.*, 2011, **36**, 1558–1628.
- 5 V. Alvarado and E. Manrique, *Energies*, 2010, **3**, 1529–1575.
- 6 S. Thomas, *Oil Gas Sci. Technol.*, 2008, **63**, 9–19.
- 7 X. Kang, J. Zhang, F. Sun, F. Zhang, G. Feng, J. Yang, X. Zhang and W. Xiang, in *Society of Petroleum Engineers, Proceedings of SPE Enhanced Oil Recovery Conference*, Kuala Lumpur, Malaysia, 2011.
- 8 V. C. Santanna, F. Curbelo, T. C. Dantas, A. D. Neto, H. S. Albuquerque and A. Garnica, *J. Pet. Sci. Eng.*, 2009, **66**, 117–120.
- 9 D. Wang, J. Cheng, Q. Yang, W. Gong, L. Qun and F. Chen, in *Society of Petroleum Engineers, Proceedings of SPE Annual Technical Conference and Exhibition*, Dallas, Texas, 2000.
- 10 H. Yang, C. Britton, P. J. Liyanage, S. Solairaj, D. H. Kim, Q. P. Nguyen, U. Weerasooriya and G. A. Pope, in *Society of Petroleum Engineers, Proceedings of SPE Improved Oil Recovery Symposium*, Oklahoma, USA, 2010.
- 11 H. Liu, C. Xiong, Z. Tao, Y. Fan, X. Tang and H. Yang, *RSC Adv.*, 2015, **5**, 33083–33088.
- 12 D. A. Z. Wever, F. Picchioni and A. A. Broekhuis, *Ind. Eng. Chem. Res.*, 2013, **52**, 16352–16363.
- 13 G. A. Pope, *J. Pet. Technol.*, 2011, **63**, 65–68.
- 14 D. A. Z. Wever, L. M. Polgar, M. C. A. Stuart, F. Picchioni and A. A. Broekhuis, *Ind. Eng. Chem. Res.*, 2013, **52**, 16993–17005.
- 15 Z. Ye, G. Gou, S. Gou, W. Jiang and T. Liu, *J. Appl. Polym. Sci.*, 2013, **128**, 2003–2011.
- 16 S. Gou, Y. He, Y. Ma, S. Luo, Q. Zhang, D. Jing and Q. Guo, *RSC Adv.*, 2015, **5**, 51549–51558.
- 17 B. Shaker Shiran and A. Skauge, *Energy Fuels*, 2013, **27**, 1223–1235.
- 18 H. Gong, L. Xu, G. Xu, M. Dong and Y. Li, *Ind. Eng. Chem. Res.*, 2014, **53**, 4544–4553.
- 19 J. Huang, X. Li and Q. Guo, *Eur. Polym. J.*, 1997, **33**, 659–665.
- 20 G. A. Stahl and D. N. Schulz, *Water-soluble Polymers for Petroleum Recovery*, Springer, 2012.
- 21 C. L. McCormick, T. Nonaka and C. B. Johnson, *Polymer*, 1988, **4**, 731–739.
- 22 C. Zhong, P. Luo, Z. Ye and H. Chen, *Polym. Bull.*, 2009, **62**, 79–89.
- 23 L. Jia, L. Yu, R. Li, X. Yan and Z. Zhang, *J. Appl. Polym. Sci.*, 2013, **130**, 1794–1804.
- 24 A. D. Child and J. R. Reynolds, *Macromolecules*, 1994, **27**, 1975–1977.
- 25 S. Gou, M. Liu, Z. Ye, L. Zhou, W. Jiang, X. Cai and Y. He, *J. Appl. Polym. Sci.*, 2014, **131**, 4221–4230.
- 26 M. Bao, Q. Chen, Y. Li and G. Jiang, *J. Hazard. Mater.*, 2010, **184**, 105–110.
- 27 J. H. Canton, W. Slooff, H. J. Kool, J. Struys, T. J. Pouw, R. Wegman and G. J. Piet, *Regul. Toxicol. Pharmacol.*, 1985, **5**, 123–131.
- 28 D. Feidieker, P. Kämpfer and W. Dott, *FEMS Microbiol. Ecol.*, 1994, **15**, 265–278.
- 29 J. A. de Bont, M. J. Vorage, S. Hartmans and W. J. Van den Tweel, *Appl. Environ. Microbiol.*, 1986, **52**, 677–680.
- 30 L. Wang, Q. Zhou, B. S. Zhang, Z. L. Li, H. Chua and D. M. Ren, *J. Environ. Sci. Health, Part A*, 2003, **38**, 1837–1848.
- 31 J. Zhong, S. Li, Y. Wei, Z. Peng and H. Yu, *J. Appl. Polym. Sci.*, 1999, **73**, 2863–2867.
- 32 I. Klari, N. S. Vrande I and U. Roje, *J. Appl. Polym. Sci.*, 2000, **78**, 166–172.
- 33 M. S. Karthikeyan, B. S. Holla and N. S. Kumari, *Eur. J. Med. Chem.*, 2007, **42**, 30–36.
- 34 K. Liu, *Carbohydr. Polym.*, 2015, **117**, 996–1001.

- 35 K. Mathauer, T. Schneider, R. Widmaier, A. Kamm and C. Bell, *US Pat.*, 10/571,937, 2004.
- 36 A. Mehrdad, I. Talebi and M. R. Rostami, *J. Chem. Eng. Data*, 2011, **56**, 3029–3037.
- 37 M. Siddiq, K. C. Tam and R. D. Jenkins, *Colloid Polym. Sci.*, 1999, **277**, 1172–1178.
- 38 P. Reuschenbach, U. Pagga and U. Strotmann, *Water Res.*, 2003, **37**, 1571–1582.
- 39 OECD 301 A-F, in *OECD Guideline for Testing of Chemicals*, Organization for Economic Co-operation and Development, Paris, 1992.
- 40 S. Gou, T. Yin, Q. Xia and Q. Guo, *RSC Adv.*, 2015, **5**, 32064–32071.
- 41 H. Frampton, J. C. Morgan, S. K. Cheung, L. Munson, K. T. Chang and D. Williams, in *Society of Petroleum Engineers, Proceedings of SPE/DOE Symposium on Improved Oil Recovery*, Tulsa, Oklahoma, 2004.
- 42 A. M. S. Maia, R. Borsali and R. C. Balaban, *Mater. Sci. Eng., C*, 2009, **29**, 505–509.
- 43 Y. Guo, Y. Liang, X. Yang, R. Feng, R. Song, J. Zhou and F. Gao, *J. Appl. Polym. Sci.*, 2013, **131**, 40633.
- 44 S. Ma, M. Liu and Z. Chen, *J. Appl. Polym. Sci.*, 2004, **93**, 2532–2541.
- 45 P. Liu, L. Zhou, C. Yang, H. Xia, Y. He and M. Feng, *J. Appl. Polym. Sci.*, 2015, **132**, 41536.
- 46 N. Hameed, J. Liu and Q. Guo, *Macromolecules*, 2008, **41**, 7596–7605.
- 47 R. Xiong, N. Hameed and Q. Guo, *Carbohydr. Polym.*, 2012, **90**, 575–582.
- 48 A. A. Chialvo, P. T. Cummings, J. M. Simonson and R. E. Mesmer, *J. Chem. Phys.*, 1999, **110**, 1064–1074.
- 49 E. E. Tucker, E. H. Lane and S. D. Christian, *J. Solution Chem.*, 1981, **10**, 1–20.
- 50 E. Jiménez-Regalado, J. Selb and F. O. Candau, *Langmuir*, 2000, **16**, 8611–8621.
- 51 Z. Ye, M. Feng, S. Gou, M. Liu, Z. Huang and T. Liu, *J. Appl. Polym. Sci.*, 2013, **130**, 2901–2911.